Geosci. Model Dev. Discuss., 5, 2811–2842, 2012
www.geosci-model-dev-discuss.net/5/2811/2012/
doi:10.5194/gmdd-5-2811-2012

Geoscientific
Model Development
Discussions

Simulations of the Mid-Pliocene Warm Period using the NASA/GISS ModelE2-R Earth System Model

M. A. Chandler[1,2], L. E. Sohl[1,2], J. A. Jonas[1,2], and H. J. Dowsett[3]

[1]Center for Climate Systems Research at Columbia University, New York, New York, USA
[2]NASA Goddard Institute for Space Studies, New York, New York, USA
[3]Eastern Geology & Paleoclimate Science Center, US Geological Survey, Reston, Virginia, USA

Received: 31 July 2012 – Accepted: 20 August 2012 – Published: 13 September 2012

Correspondence to: M. A. Chandler (mac59@columbia.edu)

Published by Copernicus Publications on behalf of the European Geosciences Union.

Abstract

Climate reconstructions of the mid-Pliocene Warm Period (mPWP) bear many similarities to aspects of future global warming as projected by the Intergovernmental Panel on Climate Change. In particular, marine and terrestrial paleoclimate data point to high latitude temperature amplification, with associated decreases in sea ice and land ice and altered vegetation distributions that show expansion of warmer climate biomes into higher latitudes. NASA GISS climate models have been used to study the Pliocene climate since the USGS PRISM project first identified that the mid-Pliocene North Atlantic sea surface temperatures were anomalously warm. Here we present the most recent simulations of the Pliocene using the AR5/CMIP5 version of the GISS Earth System Model known as ModelE2-R. These simulations constitute the NASA contribution to the Pliocene Model Intercomparison Project (PlioMIP) Experiment 2. Many findings presented here corroborate results from other PlioMIP multi-model ensemble papers, but we also emphasize features in the ModelE2-R simulations that are unlike the ensemble means. We provide discussion of features that show considerable improvement compared with simulations from previous versions of the NASA GISS models, improvement defined here as simulation results that more closely resemble the ocean core data as well as the PRISM3D reconstructions of the mid-Pliocene climate. In some regions even qualitative agreement between model results and paleodata are an improvement over past studies, but the dramatic warming in the North Atlantic and Greenland-Iceland-Norwegian Sea in these new simulations is by far the most accurate portrayal ever of this key geographic region by the GISS climate model. Our belief is that continued development of key physical routines in the atmospheric model, along with higher resolution and recent corrections to mixing parameterizations in the ocean model, have led to an Earth System Model that will produce more accurate projections of future climate.

1 Introduction

General circulation model simulations have been used to explore the Pliocene as a potential future climate analog since NASA and the USGS partnered on a data-model comparison project in the early 1990's (Rind and Chandler, 1991; Chandler and Rind, 1992; Chandler et al., 1994; Poore and Chandler, 1994). However, those studies have often had difficulty in reproducing the high degree of polar amplification seen in Pliocene data, particularly in the North Atlantic Ocean, without resorting to levels of CO_2 that are extreme and which are not supported by proxy data (Hansen and Sato, 2012; Pagani et al., 2010; Seki et al., 2010). To further complicate the issue, higher CO_2 levels lead to low-latitude sea surface temperature increases that are not supported by an increasing number of ocean core analyses from tropical locations, a finding which largely validates prior assertions that the Pliocene tropical sea surface temperatures (SSTs) were little changed from the modern. Still, the ability to compare warm-climate simulations with data-supported global reconstructions is an advantage that is not afforded by future climate change scenarios. Many groups therefore continue to pursue a better understanding of the middle Pliocene as it provides climate scientists with one of the few warm-climate scenarios in which global and high-latitude temperatures were as warm as IPCC's future climate projections, and has continental and ocean basin configurations that approximate modern geography.

The experiments examined in this study were performed in conjunction with the Pliocene Model Intercomparison Project (PlioMIP) Phase 1, and represent experiment 2, the coupled ocean-atmosphere simulation. A description of the experiment design can be found in Haywood et al. (2010, 2011). Specific model characteristics that affect experiment design and which are unique to the NASA GISS modeling effort are described below.

2 PlioMIP experiment design

For PlioMIP, a set of environmental reconstructions of the mid-Piacenzian Stage was compiled to form the PRISM3D reconstruction (Dowsett et al., 2010). These reconstructions are distributed by the US Geological Survey as a series of uniformly gridded (2° × 2°) data sets, and constitute the preferred PlioMIP experiment protocol (Haywood et al., 2010, 2011). The adaptation of these data sets into boundary conditions for use with GISS ModelE2, as well as the creation of required related inputs, is described below.

2.1 Land/ice topography and ocean bathymetry

A reconstructed topography and land/sea mask for the Pliocene (Sohl et al., 2009), reflecting a 25-m rise in sea level compared to the modern, was developed as part of the PRISM3D effort. Elevation and areal distribution information for static representations of the Greenland Ice Sheet and East Antarctic Sheet (Hill et al., 2007) are incorporated into the topography, as the ice sheets must essentially represented as "big white plateaus" for models that do not have dynamic land ice capabilities. The original 2° × 2° PRISM3D gridded topographic data set was regridded in two ways for use with GISS ModelE2: once to 2° latitude × 2.5° longitude for the atmosphere component of the model, and further to 1° latitude × 1.25° longitude for the ocean component. Corrections to the resulting land-sea masks at both resolutions were made by hand to ensure that continental outlines were consistent after regridding, that larger islands did not disappear as a result of the interpolation used in the regridding process, and that narrow ocean passages that existed in the Pliocene remained open. In ModelE2, a straits parameterization is used to keep some open ocean area in grid cell locations where straits cannot be resolved at the 1° × 1.25° resolution of the land/sea mask in the ocean component of the model; this was also modified for our Pliocene simulations (see Table 1 for a comparison to the modern).

Note that the entire West Antarctic Ice Sheet is absent in our reconstruction (as per Pollard and DeConto, 2009), creating an “Ellsworth Passage” that separates the modern Antarctic Peninsula from the rest of Antarctica. The Pliocene ocean bathymetry in this region is uncertain, since we do not know what the thickness of any previous West Antarctic Ice Sheet may have been, nor whether the region was still undergoing glacio-isostatic adjustment after the loss of such ice. The current depth to bedrock in the region varies from 500 to 2000 m (Lythe et al., 2000); we used a uniform depth of approximately 500 m as a reasonable estimate for maximum ocean depth through the passage during the Pliocene.

Ocean bathymetry for the Pliocene was otherwise adapted from the modern, with most modifications made to accommodate continental edges flooded by the increase in sea level.

2.2 Riverflow and continental drainage

The river drainage system of the continents for the Pliocene experiments is similar to that of modern geography, but exceptions exist that cannot be prescribed based on the available paleogeographic evidence. For example, adjustments related to the coastal slope changes are required due to the sea level rise of 25 m, which was prescribed as consistent with reductions of ice sheet volume. Using the topographic elevation boundary condition array, and working inward from continental edges, we calculate the slope of each continental grid cell in eight directions (four sides, four corners). Runoff is then removed from each cell in the direction of maximum slope, tracing a route back to the coast. For coastal grid cells that have more than one border adjacent to an ocean grid cell, runoff crosses the coastal grid cell on the same trajectory as in the adjacent inland grid cell.

Glacial ice melts directly from the Greenland and East Antarctic ice sheets, and enters the surface ocean in prescribed cells wherever the edges of the ice sheets coincide with continental edges.

2.3 Ocean temperatures and salinity

Both the sea surface and deep ocean temperature data sets provided with PRISM3D were regridded to 1° latitude × 1.25° longitude horizontal resolution; the vertical resolution of the deep ocean temperature data set was maintained at 33 layers. Wherever there were missing values within the regridded temperature data set with respect to our new ocean bathymetry, we used a "nearest neighbor" approach to fill the gaps, always maintaining the integrity of the vertical temperature profile. Salinity values for the Pliocene were derived from modern salinity values (Conkright et al., 1998), with missing values filled in in the same fashion as the temperatures.

2.4 Biome distribution mapping to GISS ModelE2 vegetation categories

GISS ModelE2 uses a vegetation scheme that includes eight vegetation types, plus land ice as an additional type. Each type is used in to define or modify certain physical characteristics of the land surface and ground, such as visible and near-infrared surface albedo, the water holding capacity of soil layers, transpiration rates, and snow masking depths. The GISS vegetation categories were originally distilled from a more detailed global vegetation compilation of Matthews (1983, 1984), and subsequently have been modified to better reflect agricultural coverage and its impact. Irrigation effects are not included. The GISS EaSM's radiation code also accounts separately for subgrid-scale fractions of bare ground in each cell.

The prescribed Pliocene biome distributions for PlioMIP were developed by the British Antarctic Survey (BAS biomes and mega-biomes; Salzmann et al., 2008), with each participating modeling group being responsible for developing a method of translation appropriate for their model's vegetation parameterization. To make this translation for the GISS model, we regridded the BAS modern mega-biome distribution to 2° latitude × 2.5° longitude (the standard resolution for the ModelE2 vegetation input), and then compared the BAS distribution cell by cell against the GISS modern vegetation distribution used for ModelE2. We then used a frequency distribution chart plotting

BAS vs. GISS types to identify dominant links between types (see Table 2), and the BAS Pliocene mega-biome distribution was translated accordingly, with non-fractional values assigned to each cell. Note that under this translation scheme, the GISS vegetation types shrub/grassland and tree/grassland have no clear corollary to the BAS mega-biomes, and instead are represented by grassland alone.

2.5 NASA-GISS ModelE2-R, CMIP5

The EaSM that we used for these simulations was developed at the NASA Goddard Institute for Space Studies (GISS). It is the AR5/CMIP5 version of the NASA GISS model, and is archived as GISS ModelE2-R (Schmidt et al., 2012). ModelE2 is the most recent version of the GISS ModelE, which was used to conduct the IPCC AR4 (Schmidt et al., 2006) climate simulations, and is the same code lineage as earlier GISS models referred to in the literature as si1997 to si2000 (e.g. Hansen et al., 2000, 2002). ModelE2 calculates temperature, pressure, winds, and specific humidity as prognostic variables, using the conservation equations for mass, energy, momentum and moisture. The standard configuration produces global climate simulations at a latitude × longitude resolution of 2.0° × 2.5° in the atmosphere, 1.0° × 1.25° in the ocean, and includes 40 layers in the atmosphere and 33 layers in the fully coupled dynamic ocean (Russell et al., 1995). ModelE2 uses second-order differencing schemes in the momentum and mass equations and a quadratic-upstream scheme for heat and moisture advection, which implicitly enhances an absolute model resolution of 2.0° × 2.5° grid to 0.7° × 0.8° (Schmidt et al., 2006, Table 1). The radiation physics includes calculations for trace gas constituents (CO_2, CH_4, N_2O, CFCs, O_3) and aerosols (natural and anthropogenic) and is capable of simulating the effects of large forcing changes in constituents such as volcanic aerosols and greenhouse gases. The forcings are assigned at startup or can be altered transiently throughout an experiment. In addition, a parameterized gravity wave drag formulation incorporates gravity-wave momentum fluxes that result from flow over topography, wind shear and convection. The generation, propagation and drag are all a function of the calculated variables at each grid box for the various vertical levels. New to this model is the capability of running with interactive atmospheric chemistry, aerosols and dust concentrations, as well as the incorporation of a model-calculated (rather than parameterized) first aerosol indirect effect. ModelE2 also employs a prognostic cloud water parameterization (Del Genio et al., 1996; Schmidt et al., 2006, 2012) that represents all important microphysical processes.

3 Sea surface and surface air temperature response

The most fundamental mismatch between warm climate paleoclimate simulations and paleoclimate proxy data has been the inability of simulations to achieve both a reduced pole-to-equator temperature gradient along with acceptable magnitudes of polar and tropical temperature amplification. Excessive greenhouse gas (GHG) levels have traditionally been required for climate models to achieve polar temperature amplification that is in the vicinity of the observed levels for the warmer time periods in Earth history. However, that same GHG excess tends to cause tropical temperatures that are unrealistically high.

Pliocene simulations are no different in this respect, including those for PlioMIP Experiment 2 (reference Haywood article in this volume). However, PlioMIP Pliocene experiments prescribe the use of 405 ppmv CO_2, with other greenhouse gases held at pre-industrial levels. Though 405 ppmv is actually on the upper end of proxy-based estimates for the Pliocene (Kürschner et al., 1996; Raymo et al., 1996; Pagani et al., 2010), that level is relatively low from the perspective of other warm Tertiary and Mesozoic climates. The problem of tropical temperature amplification in Pliocene simulations is thus less of a conundrum than for most past warm periods. All the same, the warming in mid- to high latitudes is supplemented substantially by the direct forcing and feedbacks associated with the additional carbon dioxide; 405 ppmv is, after all, 45 % higher than the 280 ppmv value used in most pre-industrial control runs. Of course, high-latitude temperatures are impacted by the specified sea ice and ice sheet distributions, which are substantially decreased compared with the present day (Hill et al., 2007); however, compared to the CMIP3 model results and previous GISS model simulations of the Pliocene (e.g. Chandler et al., 1994; Shukla et al., 2009, 2011; Haywood et al., 2012), the CMIP5 version of the GISS ModelE2 EaSM shows compelling improvement. In the final analysis, the coupled ocean-atmosphere simulation results (PlioMIP Experiment 2) and those from the specified SST simulation (PlioMIP Experiment 1) resemble each other beyond the results of any of our previous studies.

3.1 Zonal average temperatures

Zonal average surface air temperature (SAT) anomalies for the Pliocene simulation peak over the regions of sea ice loss and ice sheet reduction, and are slightly warmer than the multi-model ensemble averages for all PlioMIP models in both the Northern (+8.2 °C) and Southern (+9.1 °C) Hemispheres (Fig. 1 and Haywood et al., 2012). High latitude amplification of sea surface temperatures (SSTs) is asymmetrical, with more than twice as much warming in the Northern Hemisphere (+4.5 °C) as in the Southern Hemisphere (+2.2 °C). The peak of the zonal average SST falls at 65° N, at the high end of the range of PlioMIP models, and slightly exceeds the PRISM3D data for that latitude. However, it is a substantial improvement on previous simulations using the NASA/GISS family of models, which were typically far too cool at high northern latitudes. The peak SST warming in the Southern Ocean and the 1–2 °C zonal average increase across southern mid-latitudes is broadly similar to proxy data in the region, which show little longitudinal variation and yield temperature increases in the same range.

Tropical zonal average SAT anomalies are approximately 1.1 °C and sea surface temperatures in the tropics are similarly amplified, with a zonal average warming of 1.2 °C just north of the equator. These values fall on the low side of the range of PlioMIP model results for the region, but remain a bit warmer than the PRISM3D reconstruction, which is barely elevated above late 20th century tropical temperatures within 10° of the equator.

3.2 Regional temperature changes: North Atlantic and Arctic Oceans

Despite minor differences in the zonal average anomalies compared to previous GISS model simulations, the zonal values are soundly within the range defined by the PlioMIP model ensemble for zonal temperature results. However, examination of the regional temperature fields shows significant basin-to-basin differences and substantial improvements over previous GISS studies, and even compared with the PlioMIP ensemble. Figure 2 draws attention to the dominant regional temperature anomalies of the North Atlantic Ocean and their extension into the Greenland-Iceland-Norwegian (GIN) and Labrador Seas. An intense SST warming occurs in the Norwegian and Iceland sectors of the GIN Sea, peaking at 9.7 °C, and the positive anomaly extends uninterrupted to south of Greenland into the Labrador Sea, including a peak exceeding 6 °C in the Atlantic Ocean east of Newfoundland.

The warm anomaly in the GIN Sea spreads southward, following the return flow of the North Atlantic gyre as it merges with the Canary Current. The peak SST values in the simulation are however only about half as large in this region as in the PRISM3D data (3–4 °C as opposed to 6–8 °C), although further north the peak values more closely resemble the data, and are 2–3X higher than the multi-model ensemble mean. In comparing the simulated warming to the core data poleward of 75° N, the model warming is also 2–4 °C too cool, but again the new simulations compare far more favorably to data reconstructions than Pliocene simulations that were run with CMIP3 versions of the GISS model.

In stark contrast, the most pronounced negative temperature anomaly in the Pliocene ocean also lies in the North Atlantic. A region of cooling, narrow in latitudinal extent but spanning nearly the width of the Atlantic Ocean, traces the regional expression and extent of the modern Gulf Stream Current (Fig. 3). Negative temperature anomalies, or regions of delayed warming, are a recurrent feature found in the North Atlantic of many warm-climate coupled model simulations, including the PlioMIP ensemble simulations and the future climate change simulations documented in the IPCC's Fourth Assessment Report (AR4; IPCC, 2007). In addition, the North Atlantic is one of the few regions where inter-model standard deviation exceeds the mean of the multi-model ensembles (Haywood et al., 2012; Meehl et al., 2007, see Figs. 10.8 and 10.9) revealing just how much our best models differ, and how great the uncertainty is regarding climate change in this critical region.

It is not surprising then that simulations of the mid-Pliocene conducted using coupled ocean-atmosphere models have rarely achieved adequate simulations of the North Atlantic Ocean. Ocean core data, and therefore PRISM3D reconstructions, have shown with considerable confidence that the North Atlantic and northward extensions into the GIN Sea experienced strong warming in the Pliocene – stronger than anywhere else in the global oceans – a result that is in marked contrast to the cooling typically seen in model simulations. Dowsett et al. (2012) point out that even accounting for a cool bias in the models compared to their own preindustrial control simulations, coupled models underestimate North Atlantic warming in the mid-Pliocene by 2–8 °C (see Fig. 2 and figures in Haywood et al., 2012).

3.3 Regional ocean temperature changes: North Pacific, Southern Ocean, and the Tropics

Temperature change throughout the rest of the global oceans is muted by comparison with the North Atlantic and Arctic, but there are still significant anomalies that can be compared and contrasted to data reconstructions in other key oceanic regions. Both the North Pacific and Southern Ocean show warming in the Pliocene simulations, but peak at lower latitudes than the Atlantic. Also unlike the Atlantic anomalies, the sea surface temperatures in the Pacific and Southern Oceans are broad and peak below +3 °C. There are less extensive, but more extreme anomalies near the Asian shoreline in the northwest Pacific, which are supported by ocean core data that Dowsett et al. (2012) given a confidence rating of “Very High”. However, it is noteworthy that the temperature anomaly lessens poleward of 45° N latitude and into the northeastern Pacific Ocean. While data from the Gulf of Alaska do not dispute that trend, cores taken off the west coast of North America, and given a “high-confidence” rating in PRISM project analyses, indicate levels of Pliocene warming that are not simulated by the model.

While mid- to high-latitude warming is evident in ocean cores throughout the Southern Ocean there is little longitudinal variation in the warming – despite the absence of the West Antarctic Ice Sheet in the Pliocene boundary conditions. ModelE2, like the multi-model PlioMIP ensemble, shows that the South Atlantic and southern Indian Ocean regions are somewhat warmer than the corresponding latitudes in the South Pacific. This feature tends to be robust, and is also borne out by the PRISM3D reconstructions.

Tropical temperature change, as mentioned previously, has proven to be a dilemma for nearly every model-data comparison for past warm periods in Earth history. The overarching theme from proxy studies is that tropical temperatures are not sensitive to the forcings and feedbacks that have driven the vast majority of past warm climates. In contrast, climate models show that when the forcing is either a well-mixed greenhouse gas or the result of changes to solar insolation, tropical temperatures respond measurably.

The mid-Pliocene, with its relatively lower levels of atmospheric CO_2 (compared to earlier warm periods in geologic history), has minimal additional forcing in the tropics, thus tropical SSTs and surface air temperatures warm only about 1 °C. Results from the PRISM analyses show that some tropical regions may in fact have experienced warming on that order (1–2 °C), but they also include a number of sites where no temperature increases are discernable. In each ocean basin, the sites that show little or no temperature change are in the central or western warm pools, whereas those sites with minor warming are generally in the easternmost portions of the basins. The ModelE2-R simulation results show generally uniform east-west temperature increases across all ocean basins and, where minor variations exist, there is no consistent east-west trend.

3.4 Arctic sea ice

The impact of the Pliocene warming on Arctic sea ice is of special interest because of the continuing degradation of the present-day polar cryosphere related to greenhouse warming. Coupled model experiments calculate rather than specify the sea ice distribution, and although the initial conditions for these simulations include reduced ice, it is not clear that models can maintain such distributions under the 405 ppmv CO_2 levels used in the PlioMIP experiments. In the case of the ModelE2-R experiments, however, the reduction is at least partially sustained: sea ice is reduced by 40 % in the Northern Hemisphere (Table 3), a significantly greater amount than the 23 % reduction of Southern Ocean sea ice, despite the latter region's lower latitude position and thinner seasonal ice pack. Reductions of Arctic sea ice are naturally greatest in the proximity of the GIN Sea warming, but decreases in sea ice are pronounced in all marginal regions of the Arctic ice cap (Fig. 4).

A further examination of the vertical temperature profile in the Atlantic and Arctic sector (Fig. 5) also shows that the remaining Arctic sea ice may be extremely vulnerable to even small amounts of additional warming. The Arctic Ocean warms considerably at depth and the sea ice cap thins dramatically as its areal coverage is reduced. No doubt this result is highly sensitive to the ocean-ice parameterization in the climate model. We explore that issue, along with the seasonal cycle of polar sea ice, in greater detail in a forthcoming paper.

3.5 Atlantic meridional overturning circulation

The most noticeable improvement of the ModelE2-R Pliocene simulations, over previous GISS model results, is the characteristic of the meridional overturning in the Atlantic Ocean. The Atlantic mass stream function is shown in Fig. 6 for both the preindustrial control and the Pliocene simulation. The peak overturning increases from 14.35 to 19.53 Sverdrups, a strengthening of the circulation by more than 35 %, and the geographic location of the peak shifts poleward by 5–10° latitude. Also apparent is the formation of an overturning cell at about 70° N, which appears to derive deep water production from either the anomalously warm Iceland or Norwegian Seas (or both). Taken together with the vertical temperature profile shown in Fig. 5, this newly developed overturning cell may be the origin of warming ocean waters at depth in the Arctic Ocean. Further sensitivity experiments will be required to examine to what extent these features are driven by the reduction of the Greenland Ice Sheet and by changes to freshwater flux associated with altered river drainage basins, and what affect the 25-m sea level rise may have had on flow through a variety of ocean straits.

4 Hydrology

In most warm climate scenarios, the hydrological cycle strengthens as more water is evaporated from the oceans and the water holding capacity of the atmosphere increases. Surface heating destabilizes air masses, increasing convective events leading to increases in precipitation rate, punctuated by longer periods of drying over land. In the Pliocene both precipitation and evaporation rates increase globally. However, the precipitation rates over land actually increase more than evaporation rates do, leading to a net moisture gain of approximately 15 % over continents. At the same time, Fig. 7 clearly shows that the geographic distribution of precipitation and evaporation changes over land are highly variable and local effects dominate the moisture balance. The vast majority of continental regions show that increased rainfall is offset by evaporation increases; similarly, decreasing precipitation over land is commonly accompanied by decreasing evaporation rates in the same region.

Across the oceans, however, this is not necessarily true. In particular, the subtropical oceans experience intensified drying, as regions where evaporation increases are also affected by declining precipitation. This effect is seen in the subtropics of the Pacific, Atlantic and Indian Oceans, as well as in both hemispheres. The implications for salinity distributions and the meridional overturning circulation may be significant. We are in the process of examining the impacts, and will discuss the findings in a future paper.

5 Discussion of global feedbacks

The primary drivers behind the climate changes simulated in the ModelE2-R Pliocene simulation are threefold: (1) altered boundary conditions, including minor modifications to continental geography and orography, coastline changes associated with a 25-m sea level rise, and the isostatic rebound of regions equilibrated to the lack of continental glaciation; (2) reduced Greenland and West Antarctic ice sheets, and the poleward extension of the Southern Ocean over West Antarctica; and (3) an increased atmospheric carbon dioxide level (405 ppmv). However, as with all warm climate experiments, the amplifying effects of feedbacks are fundamental to the evolution of the simulation and to the ultimate equilibrium state of the climate (see Table 3 and discussion below).

The global average temperature increase in the mid-Pliocene simulations compared to the pre-industrial control runs is 2.25 °C. Consistent with future climate change projections, the Northern Hemisphere warms more than the Southern Hemisphere (2.4 °C vs. 2.1 °C). Albedo changes are generally an important positive feedback in warming climates, and the reduced planetary albedo in the Pliocene simulations is consistent across both Northern and Southern Hemispheres. Of course the ground albedo change is substantial (–20% NH, −13% SH), as snow and ice cover decrease dramatically in the warmer climate. The specified reduction of ice sheets also imposes a decrease in ground albedo, although it is not as large an effect as the albedo change caused by the loss of snow and ice cover, which is calculated by the GCM. Snow depth, while decreasing in the Northern Hemisphere, actually increases on average in the Southern Hemisphere. This less obvious result is due to the great reduction in circum-Antarctic sea ice, which leads to increased evaporation across warm waters and large increases in snow accumulation over the margins of East Antarctica. The West Antarctica Ice Sheet is gone (and West Antarctica itself is mostly submerged), but sea ice formation across that high latitude ocean still forms a platform that allows snow accumulation for much of the year. This begs the question as to whether or not the GISS ModelE2-R would actually support the re-initiation or maintenance of continental glaciation on any portion of West Antarctica.

The other factor in planetary albedo change is the role of cloud cover. Total cloud cover decreases in the Pliocene, but this is not necessarily an indication of the sign of the feedback, since the vertical distribution of clouds can alter their impact on albedo. However, the vertical profile of cloud changes shown in Fig. 8 strongly suggests that clouds enhance the Pliocene warming, since they decrease on average at every level in the lower and middle troposphere, while increasing slightly near the tropopause. Moist convective cloud cover is the only cloud type to increase in the Pliocene simulations, consistent with the strengthened hydrologic cycle.

Beyond the albedo changes, the atmospheric water vapor increases by about 15 %, providing the typical amplification of the greenhouse effect and another positive feedback that maintains a warmer Pliocene climate. The increased surface area covered by water in the Pliocene plays a role in this increased atmospheric water vapor, but the negative moisture balance across the subtropical ocean expanses of the Southern Hemisphere is a key factor as well (Fig. 7). Intensification of the hydrological cycle results from increases in both rainfall and evaporation rates (+6 %) but annual average precipitation changes over most continental regions are balanced by similarly altered regional patterns of evaporation (at least in sign if not entirely in magnitude). In contrast, there are significant geographic expanses of the subtropics where both precipitation and evaporation change amplifies the effect of the other. The impact on ocean surface salinity may be important to the long-term equilibrium state of Pliocene ocean circulation; we are in the process of conducting longer integrations (beyond these 1000 yr simulations) to explore the issue.

6 Conclusions

Given its intriguing potential as a near-analogue to future climate, the mid-Pliocene Warm Period has been explored by climate modelers since the early 1990's. This interval between 3.3–3.0 million years ago may truly be the most recent global warming that is anywhere close in magnitude to what the Earth faces in its near future. Unfortunately, experiments with many of the coupled ocean-atmosphere models that IPCC relies on for future climate projections have not been able to reproduce the middle Pliocene distribution of warm sea surface temperatures, particularly the strong warming in the far North Atlantic Ocean (Haywood et al., 2012; Dowsett et al., 2012). Numerous proxy studies imply that higher CO_2 levels are not the sole answer to Pliocene warming, as prior assertions of stable tropical SSTs have been corroborated with each new low-latitude ocean core and each new proxy method.

In this paper we show preliminary results of the most recent simulations of the Pliocene Warm Period using the latest version (AR5/CMIP5) of the GISS Earth System Model, called ModelE2-R. These simulations are the NASA GISS contribution to the Pliocene Model Intercomparison Project (PlioMIP, Experiment 2) and will be used in future phases of the PlioMIP multi-model ensemble studies. Many of our results from this new simulation fall squarely within the range defined by other coupled models in the PlioMIP ensemble, but we emphasize here some features that would be outliers in the ensemble ranges. We consider many of these outlier results to be improvements, because the simulation results more closely resemble the ocean core data and PRISM3D reconstructions. The most prominent of these improvements is the simulation of a large region of warming in the North Atlantic and Greenland-Iceland-Norwegian Sea (large areas covered by SST anomalies greater than +4 °C, with distinct peaks of more than 9 °C). This is by far the most accurate portrayal of this key geographic region by any version of the NASA GISS family of models. There are still model-data differences to be addressed, and these preliminary results require further analysis in order to fully understand the physical processes involved in the warming of the North Atlantic and in the changes to ocean circulation. However, we believe that continued development of key physical routines in the GISS atmospheric model, along with higher resolution and recent corrections made to the Gent-McWilliams mixing parameterization in the

Russell ocean model, have led to an Earth System Model that will produce more accurate projections of future climate.

References

Chandler, M. A. and Rind, D.: The influence of warm North Atlantic Sea surface temperatures on the Pliocene Climate: GCM Sensitivity Experiments, EOS T. Am. Geophys. Un., 73, 169, 1992.

Chandler, M. A., Rind, D., and Thompson, R. S.: Joint investigations of the middle Pliocene climate II: GISS GCM Northern Hemisphere results, Global Planet. Change, 9, 197–219, doi:10.1016/0921-8181(94)90016-7, 1994.

Conkright, M. E., Levitus, S., O'Brien, T., Boyer, T. P., Stephens, C., Johnson, D., Stathoplos, L., Baranova, O., Antonov, J., Gelfeld, R., Burney, J., Rochester, J., and Forgy, C.: World Ocean Database 1998 Documentation and Quality Control, National Oceanographic Data Center, Silver Spring, MD, 114 pp., 1998.

Del Genio, A. D., Yao, M.-S., Kovari, W., and Lo, K. K.-W.: A prognostic cloud water parameterization for global climate models, J. Climate, 9, 270–304, doi:10.1175/1520-0442(1996)009¡0270:APCWPF¿2.0.CO;2, 1996.

Dowsett, H. J., Thompson, R. S., Barron, J. A., Cronin, T. M., Fleming, R. F., Ishman, S. E., Poore, R. Z., Willard, D. A. and Holtz, T. R.: Joint investigations of the middle Pliocene climate I: PRISM paleoenvironmental reconstructions, Global Planet. Change, 9, 169–195, 2004.

Dowsett, H., Robinson, M., Haywood, A., Salzmann, U., Hill, D., Sohl, L., Chandler, M., Williams, M., Foley, K., and Stoll, D.: The PRISM3D paleoenvironmental reconstruction, Stratigraphy, 7, 123–139, 2010.

Hansen, J. E. and Sato, M.: Paleoclimate implications for human-made climate change, in: Climate Change: Inferences from Paleoclimate and Regional Aspects, edited by: Berger, A., Mesinger, F., and Šijački, D., Springer, Vienna, Austria, doi:10.1007/978-3-7091-0973-1_2, pp. 21–48, 2012.

Hansen, J., Ruedy, R., Lacis, A., Sato, M., Nazarenko, L., Tausnev, N., Tegen, I., and Koch, D.: Climate modeling in the global warming debate, in: General Circulation Model Development, edited by: Randall, D., Academic Press, San Diego, pp. 127–164, 2000.

Hansen, J., Sato, M., Nazarenko, L., Ruedy, R., Lacis, A., Koch, D., Tegen, I., Hall, T., Shindell, D., Santer, B., Stone, P., Novakov, T., Thomason, L., Wang, R., Wang, Y., Jacob, D., Hollandsworth, S., Bishop, L., Logan, J., Thompson, A., Stolarski, R., Lean, J., Willson, R., Levitus, S., Antonov, J., Rayner, N., Parker, D., and Christy, J.: Climate forcings in Goddard Institute for Space Studies SI2000 simulations, J. Geophys. Res., 107, 4347, doi:10.1029/2001JD001143, 2002.

Haywood, A. M., Dowsett, H. J., Otto-Bliesner, B., Chandler, M. A., Dolan, A. M., Hill, D. J., Lunt, D. J., Robinson, M. M., Rosenbloom, N., Salzmann, U., and Sohl, L. E.: Pliocene Model Intercomparison Project (PlioMIP): experimental design and boundary conditions (Experiment 1), Geosci. Model Dev., 3, 227–242, doi:10.5194/gmd-3-227-2010, 2010.

Haywood, A. M., Dowsett, H. J., Robinson, M. M., Stoll, D. K., Dolan, A. M., Lunt, D. J., Otto-Bliesner, B., and Chandler, M. A.: Pliocene Model Intercomparison Project (PlioMIP): experimental design and boundary conditions (Experiment 2), Geosci. Model Dev., 4, 571–577, doi:10.5194/gmd-4-571-2011, 2011.

Haywood, A. M., Hill, D. J., Dolan, A. M., Otto-Bliesner, B., Bragg, F., Chan, W.-L., Chandler, M. A., Contoux, C., Jost, A., Kamae, Y., Lohmann, G., Lunt, D. J., Abe-Ouchi, A., Pickering, S. J., Ramstein, G., Rosenbloom, N. A., Sohl, L., Stepanek, C., Yan, Q., Ueda, H., and Zhang, Z.: Large-scale features of Pliocene climate: results from the Pliocene Model Intercomparison Project, Clim. Past Discuss., 8, 2969–3013, doi:10.5194/cpd-8-2969-2012, 2012.

Hill, D. J., Haywood, A. M., Hindmarsh, R. C. M., and Valdes, P. J.: Characterising ice sheets during the Pliocene: evidence from data and models, in: Deep-Time Perspectives on Climate Change: Marrying the Signal from Computer Models and Biological Proxies, edited by: Williams, M., Haywood, A. M., Gregory, J., and Schmidt, D., Micropalaeontol. Soc., Spec. Pub. Geol. Soc., London, pp. 517–538, 2007.

IPCC: Climate Change 2007: The Physical Science Basis. Contribution of Working Group I to the Fourth Assessment Report of the Intergovernmental Panel on Climate Change, edited by: Solomon, S., Qin, D., Manning, M., Chen, Z., Marquis, M., Averyt, K. B., Tignor, M., and Miller, H. L., Cambridge Univ. Press, Cambridge, UK, and New York, 996 p., 2007.

Kürschner, W. M., Van der Burgh, J., Visscher, H., and Dilcher, D. L.: Oak leaves as biosensors of late Neogene and early Pleistocene paleoatmospheric CO_2 concentrations, Mar. Micropaleontol., 27, 299–312, 1996.

Lythe, M. B., Vaughn, D. G., and the BEDMAP Consortium, BEDMAP – bed topography of the Antarctic, Cambridge, U. K., British Antarctic Survey, 2000. Digital media available at http://nsidc.org/data/atlas/, accessed 23 January 2011.

Matthews, E.: Global vegetation and land use: New high-resolution data bases for climate studies, J. Clim. Appl. Meteorol., 22, 474–487, doi:10.1175/1520-0450(1983)022<0474:GVALUN>2.0.CO;2, 1983.

Matthews, E.: Prescription of Land-Surface Boundary Conditions in GISS GCM II: A Simple Method Based on High-Resolution Vegetation Data Bases, NASA TM-86096, National Aeronautics and Space Administration, 1984.

Meehl, G. A., Stocker, T. F., Collins, W. D., Friedlingstein, P., Gaye, A. T., Gregory, J. M., Kitoh, A., Knutti, R., Murphy, J. M., Noda, A., Raper, S. C. B., Watterson, I. G., Weaver, A. J., and Zhao, Z.-C.: Global climate projections, in: Climate Change 2007: The Physical Science Basis. Contribution of Working Group I to the Fourth Assessment Report of the Intergovernmental Panel on Climate Change, edited by: Solomon, S., Qin, D., Manning, M., Chen, Z., Marquis, M., Averyt, K. B., Tignor, M., and Miller, H. L., Cambridge University Press, Cambridge, UK and New York, NY, USA, 747–845, 2007.

Pagani, M., Liu, Z. H., LaRiviere, J., and Ravelo, A. C.: High Earth-system climate sensitivity determined from Pliocene carbon dioxide concentrations, Nature Geosci., 3, 27–30, doi:10.1038/NGEO724, 2010.

Pollard, D. and DeConto, R. M.: Modelling West Antarctic ice sheet growth and collapse through the past five million years, Nature, 458, 329–332, 2009.

Poore, R. Z. and Chandler, M. A.: Simulating past climates. The data-model connection, Global Planet. Change, 9, 165–167, 1994.

Raymo, M. E., Grant, B., Horowitz, M., and Rau, G. H.: Mid-Pliocene warmth: Stronger greenhouse and stronger conveyor, Mar. Micropaleontol., 27, 313–326, doi:10.1016/0377-8398(95)00048-8, 1996.

Rind, D. and Chandler, M. A.: Increased ocean heat transports and warmer climate, J. Geophys. Res., 96, 7437–7461, doi:10.1029/91JD00009, 1991.

Russell, G. L., Miller, J. R., and Rind, D.: A coupled atmosphere-ocean model for transient climate change studies, Atmos. Ocean, 33, 683–730, 1995.

Salzmann, U., Haywood, A. M., Lunt D. J., Valdes, P. J., and Hill, D. J.: A new Global Biome Reconstruction and Data-Model Comparison for the middle Pliocene, Global Ecol. Biogeogr., 17, 432–447, 2008.

Schmidt, G. A., Ruedy, R., Hansen, J. E., Aleinov, I., Bell, N., Bauer, M., Bauer, S., Cairns, B., Canuto, V., Cheng, Y., Del Genio, A., Faluvegi, G., Friend, A. D., Hall, T. M., Hu, Y., Kelley, M., Kiang, N. Y., Koch, D., Lacis, A. A., Lerner, J., Lo, K. K., Miller, R. L., Nazarenko, L., Oinas, V., Perlwitz, J. P., Perlwitz, Ju., Rind, D., Romanou, A., Russell, G. L., Sato, M., Shindell, D. T., Stone, P. H., Sun, S., Tausnev, N., Thresher, D., and Yao, M.-S.: Present day atmospheric simulations using GISS ModelE: Comparison to in-situ, satellite and reanalysis data, J. Climate, 19, 153–192, doi:10.1175/JCLI3612.1, 2006.

Schmidt, G. A., Kelley, M., Nazarenko, L., Ruedy, R., Russell, G. L., Aleinov, I., Bauer, M., Bauer, S., Bhat, M. K., Bleck, R., Canuto, V., Chen, Y., Ye Cheng, Clune, T. L., Del Genio, A., de Fainchtein, R., Faluvegi, G., Hansen, J. E., Healy, R. J., Kiang, N. Y., Koch, D., Lacis, A. A., LeGrande, A. N., Lerner, J., Lo, K. K., Marshall, J., Menon, S., Miller, R. L., Oinas, V., Oloso, A. O., Perlwitz, J., Puma, M. J., Putman, W. M., Rind, D., Romanou, A., Sato, M., Shindell, D. T., Shan Sun, Syed, R. A., Tausnev, N., Tsigaridis, K., Unger, N., Voulgarakis, A., Mao-Sung, Y., Jinlun, Z.: Configuration and assessment of the GISS ModelE2 contributions to the CMIP5 archive, in preparation, 2012.

Seki, O., Foster, G. L., Schmidt, D. N., Mackensen, A., Kawamura, K., and Pancost, R. D.: Alkenone and boron-based Pliocene pCO_2 records, Earth Planet. Sc. Lett., 292, 201–211, 2010.

Shukla, S. P., Chandler, M. A., Jonas, J., Sohl, L. E., Mankoff, K., and Dowsett, H.: Impact of a permanent El Niño (El Padre) and Indian Ocean Dipole in warm Pliocene climates, Paleoceanography, 24, PA2221, doi:10.1029/2008PA001682, 2009.

Shukla, S. P., Chandler, M. A., Rind, D., Sohl, L. E., Jonas, J., and Lerner, J.: Teleconnections in a warmer climate: The Pliocene perspective, Clim. Dynam., 37, 1869–1887, doi:10.1007/s00382-010-0976-y, 2011.

Sohl, L. E., Chandler, M. A., Schmunk, R. B., Mankoff, K., Jonas, J. A., Foley, K. M., and Dowsett, H. J.: PRISM3/GISS topographic reconstruction, US Geol. Surv. Data Series, 419, 6 pp., 2009.

Table 1. Straits parameterizations in GISS ModelE2 – Modern vs. Pliocene.

Strait Name	Geographic Location	Depth (m)	Width (m)	Modern	Pliocene
Dolphin & Union	Between Victoria Island and mainland Canada, Northwest Territories/Nunavut	56	32 000	present	—
Dease	Between Victoria Island and the Kent Peninsula, Nunavut, Canada	56	25 000	present	—
Fury & Hecla	Between Baffin Island and the Melville Peninsula, Nunavut, Canada	30	15 000	present	present
Nares	Between Ellesmere Island, Canada and Greenland	202	30 000	present	present*
Gibraltar	Between Spain and Morocco	280	15 000	present	—
English	Between England and France	30	35 000	present	—
Dardanelles	Northwestern Turkey	30	1000	present	present
Bosporous	Northwestern Turkey	30	2000	present	—
Bab al-Mandab	Connects Red Sea and Gulf of Aden	140	25 000	present	present
Malacca	Between Malay Peninsula and Sumatra, Indonesia	30	40 000	present	present
Selat Sunda	Between Java and Sumatra, Indonesia	30	25 000	present	present

* The Nares Strait is divided into two parts to accommodate Pliocene geography.

Table 2. Correlation of BAS mega-biomes with GISS ModelE2 modern vegetation classes.

BAS Mega-Biome Type	GISS Vegetation Type
Tropical Forest	Rainforest
Warm-temperate forest	Deciduous forest
Savanna/dry woodland	Grassland
Grassland/dry shrub	Grassland
Desert	Desert
Temperate forest	Deciduous forest
Boreal forest	Evergreen forest
Tundra	Tundra
Dry tundra	Tundra

Table 3. Global mean climate values.

	Combined land+ocean+ice budgets					
	Global	N. Hem.	S. Hem.	Global	N. Hem.	S. Hem.
	Surface air temperature (°C)			H_2O of atmosphere (mm)		
G1 Pliocene	16.21	16.61	15.81	25.99	26.64	25.33
E148 Control	13.96	14.20	13.73	22.74	22.79	22.69
Difference	2.25	2.41	2.08	3.25	3.85	2.64
	Planetary albedo (%)			Precipitation (mm/day)		
G1 Pliocene	28.87	29.54	28.20	3.34	3.40	3.28
E148 Control	29.71	30.31	29.11	3.17	3.15	3.17
Difference	*−0.84*	*−0.77*	*−0.91*	0.18	0.25	0.11
	Snow coverage (%)			Evaporation (mm/day)		
G1 Pliocene	7.67	9.16	6.18	3.34	3.20	3.49
E148 Control	9.96	11.20	8.73	3.17	3.01	3.33
Difference	*−2.29*	*−2.04*	*−2.55*	0.18	0.19	0.16
	Snow depth (mm H_2O)			Total cloud cover (%)		
G1 Pliocene	12.80	10.11	15.49	59.51	60.53	58.50
E148 Control	10.35	14.35	6.35	61.76	62.53	61.00
Difference	2.45	*−4.24*	9.14	*−2.25*	*−2.00*	*−2.50*
	Ocean ice cover (%)			Moist convective cloud cover (%)		
G1 Pliocene	3.14	3.40	2.87	4.20	3.97	4.44
E148 Control	4.71	5.71	3.72	4.08	3.85	4.31
Difference	*−1.57*	*−2.31*	*−0.85*	0.12	0.12	0.13
	Surface ground albedo (%)					
G1 Pliocene	10.40	11.06	9.76			
E148 Control	12.43	13.68	11.20			
Difference	*−2.03*	*−2.62*	*−1.44*			

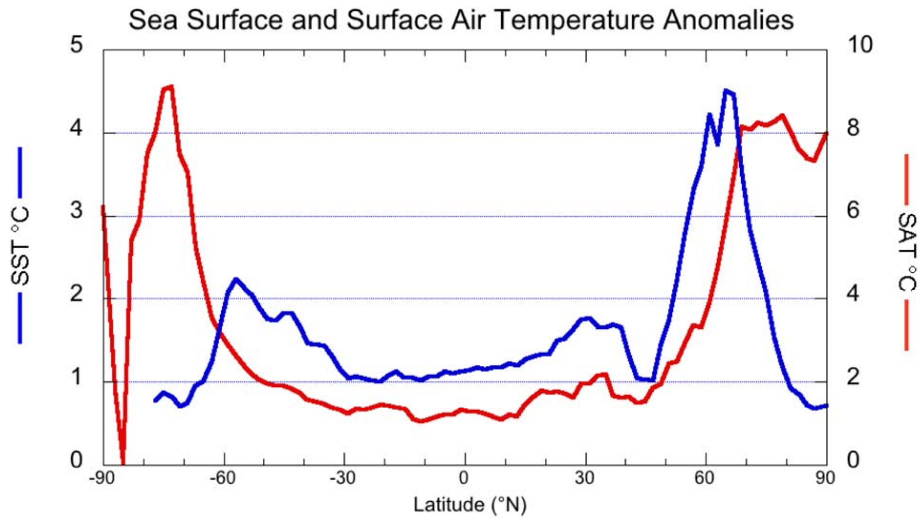

Fig. 1. Zonal average anomalies of surface air temperature (in red) and sea surface temperature (in blue). Note the dual *Y*-axis scales. The high-latitude amplification of temperature is close to that derived from data, while the peak SSTs around 65° N are not typically reproduced by coupled ocean-atmosphere models, including earlier versions of the GISS GCM. Tropical temperature anomalies are reduced compared to previous simulations but are still higher than data reconstructions for the mid-Pliocene.

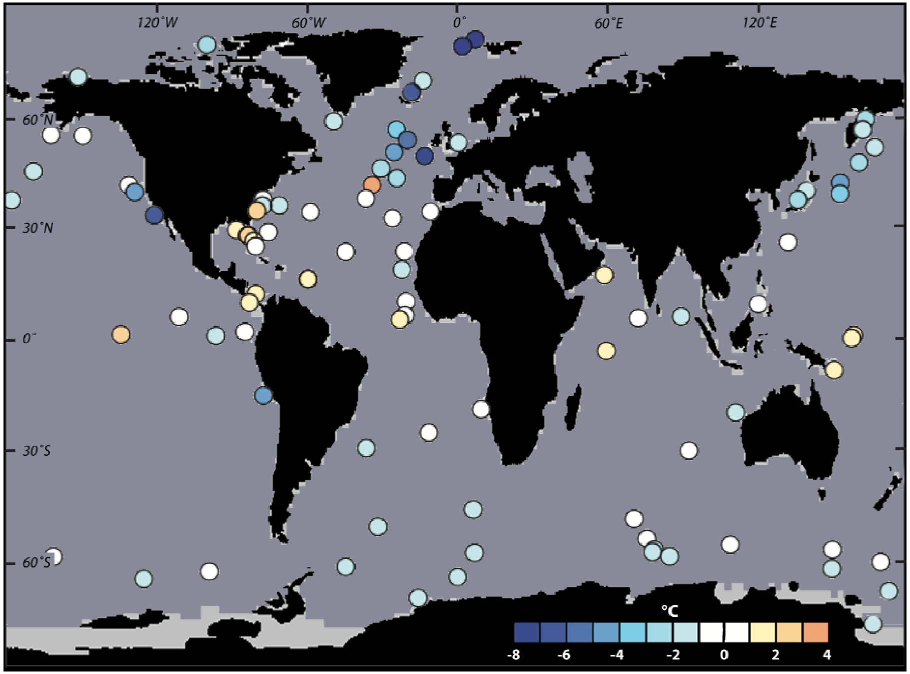

Fig. 2. Difference of the mean model sea surface temperature compared to estimates of SST from PRISM3 ocean core proxy data (data from Dowsett et al., 2012). The model mean is from a four-model subset of the PlioMIP project ensemble, which includes an earlier GISS ModelE simulation. The model results are corrected for control run biases before comparison to the ocean core data. The underestimate of North Atlantic temperature change is characteristic of problems with coupled-model comparisons to many warm climate periods in Earth's past, and in particular to the PRISM3D reconstructions of the mid-Pliocene Warm Period.

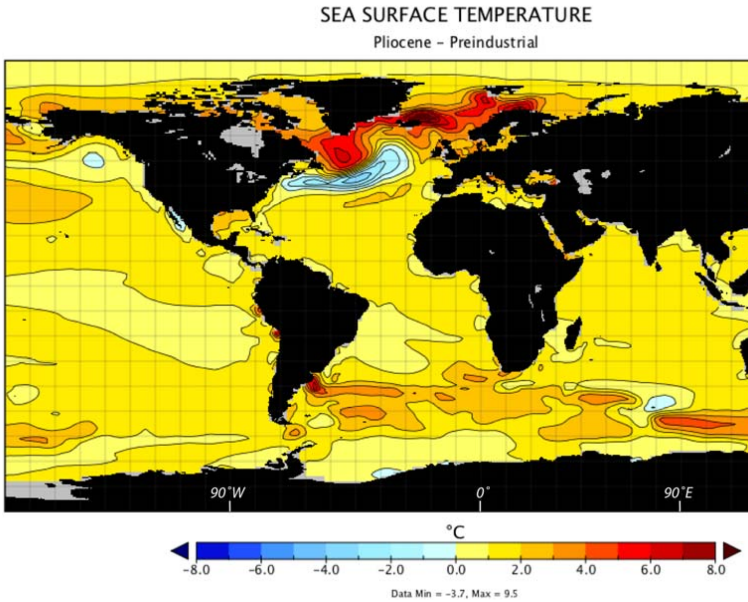

Fig. 3. The sea surface temperature anomaly field from the Pliocene simulation (compared to a pre-industrial control) shows a generally warmer planet with high-latitude amplification of SSTs. The dominant features of the field are the strong North Atlantic temperature changes, which were not found in Pliocene simulations conducted using the AR4/CMIP3 version of the GISS ModelE. The North Atlantic and Southern Ocean warm anomalies are key fingerprints of the mid-Pliocene Warm Period as reconstructed by the U.S. Geological Survey PRISM3D Project, suggesting that ModelE2-R (the AR5/CMIP5 version of the model) is superior to the previous AR4 version of the model in a key aspect.

Title Page
Abstract | Introduction
Conclusions | References
Tables | Figures
|◀ | ▶|
◀ | ▶
Back | Close
Full Screen / Esc
Printer-friendly Version
Interactive Discussion

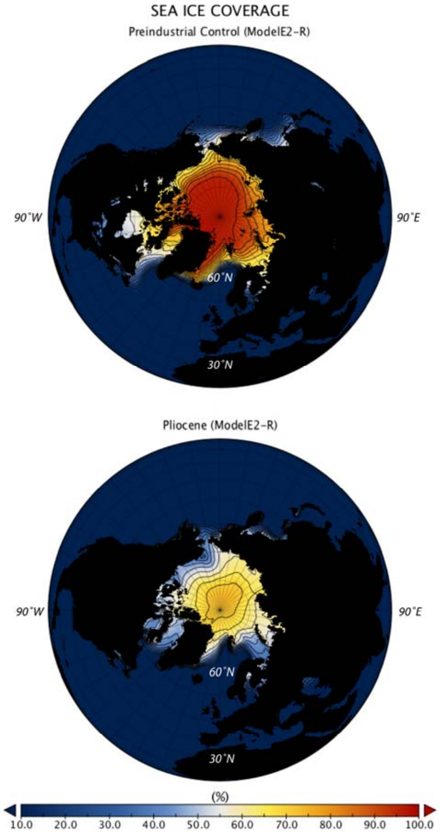

Fig. 4. Extent of sea ice cover from a preindustrial simulation (top) and the mid-Pliocene simulation (bottom). Sea ice in the Pliocene run is reduced by 40 % in the Arctic Ocean and retreats on all margins, not just in the North Atlantic where SSTs warm the most. The central Arctic ice cap in the Pliocene no longer maintains a large geographic area where ice cover is above 90 %. Ice thickness is greatly reduced as well, indicative of a loss of multi-year ice and suggesting that the region would be highly vulnerable to even moderate further increases in temperature.

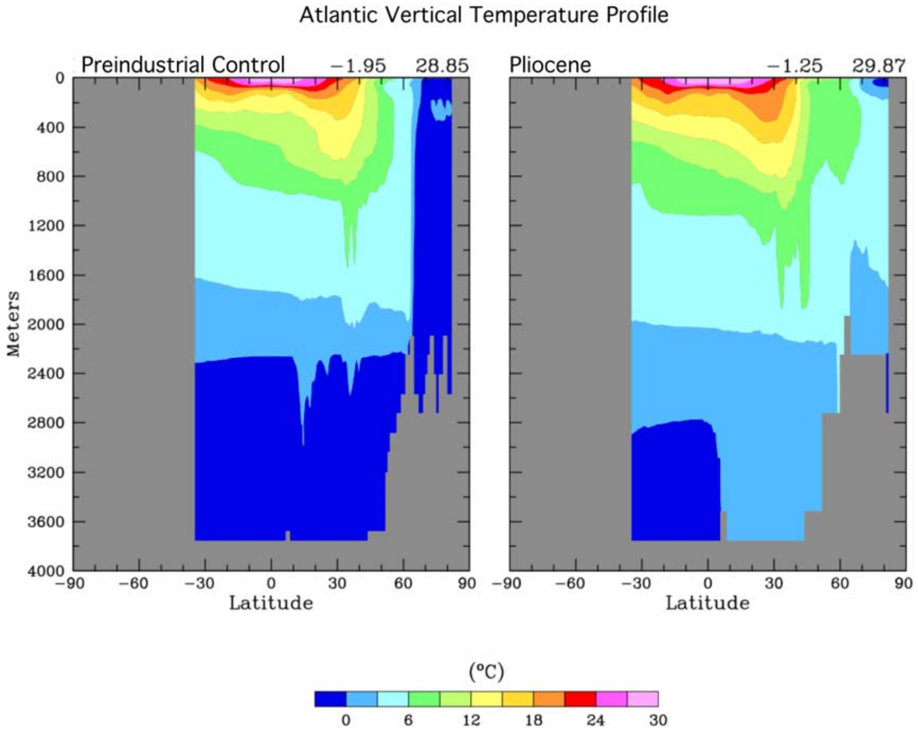

Fig. 5. The vertical profile of zonal average ocean temperatures in the Atlantic Ocean basin for the pre-industrial control run (left) and the Pliocene simulation (right). Deep and bottom water temperatures warm, associated with reductions in Antarctic Bottom Water production (not shown) and increased production of North Atlantic Deep Water (see Fig. 6 and text). Warming at depth in the Arctic Ocean is also evident, leaving sea ice at the surface even more vulnerable to melting than the substantial 40 % ice cover reduction might suggest.

Title Page
Abstract
Introduction
Conclusions
References
Tables
Figures
◀◀
▶▶
◀
▶
Back
Close
Full Screen / Esc
Printer-friendly Version
Interactive Discussion

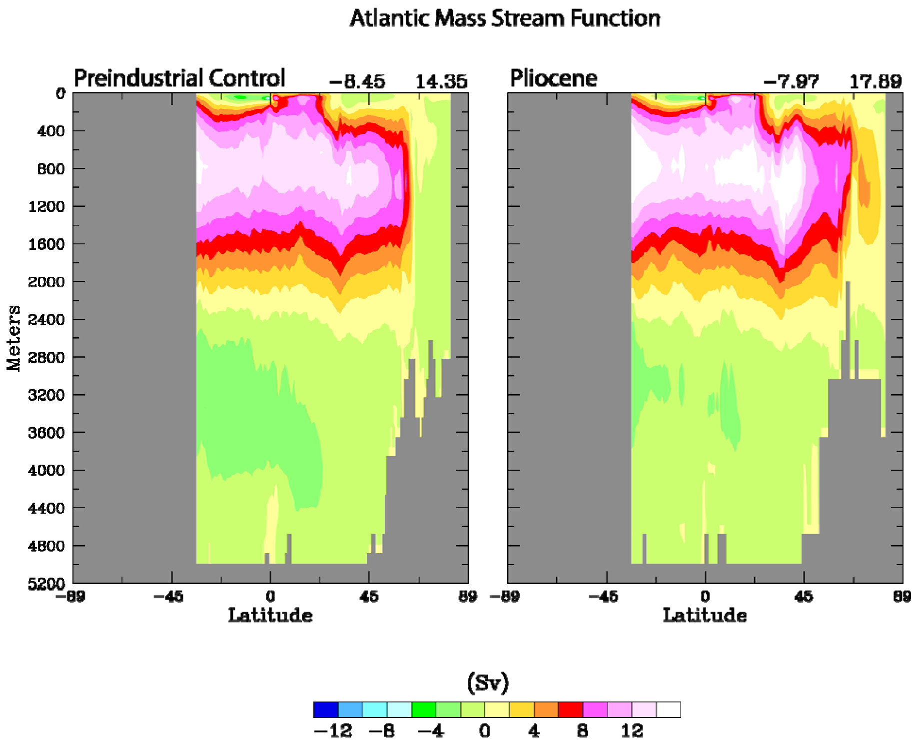

Fig. 6. Zonally averaged mass stream function in the Atlantic Ocean basin for the preindustrial run (left) and the Pliocene simulation (right). Peak overturning in the North Atlantic of the Pliocene strengthens by over 35 % compared to the preindustrial run, including an intrusion of a plume of water, with origins in the North Atlantic, to depths of over 1000 m the Arctic Ocean. This increased overturning in the Pliocene has been hypothesized for years based on surface and deep water temperature proxies and estimates of NADW penetration relative to water masses from other basins. However, coupled climate models have rarely found this feature in Pliocene experiments.

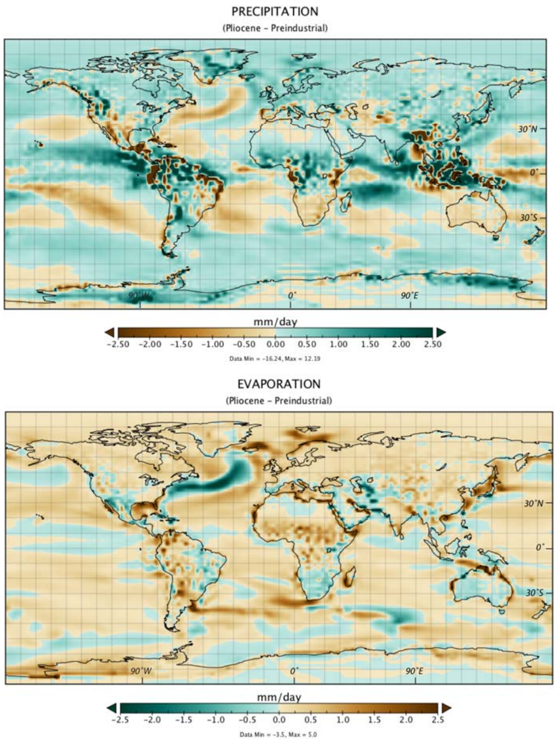

Fig. 7. Precipitation and evaporation anomaly fields for the mid-Pliocene simulation minus the pre-industrial control run. An intensified hydrological cycle is evident from global increases in both rainfall and evaporation rates. Note that the colorbars are flipped in the two maps – green shades indicate a tendency toward wetter conditions in both maps, while brown indicates drying. Most regional changes in precipitation over land are balanced by evaporation, at least in sign if not in magnitude. In contrast, there are significant regions of the ocean, especially in the subtropics, where the hydrological anomaly in both precipitation and evaporation amplifies the other. The impact on ocean surface salinity needs to be explored with further experiments and analyses.

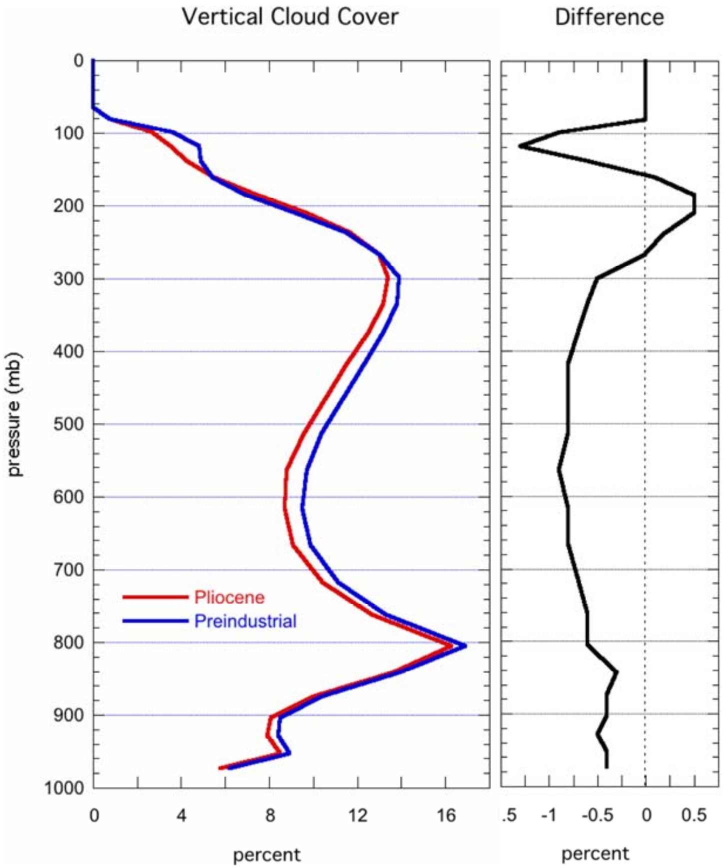

Fig. 8. The zonally averaged vertical profile of total cloud cover from the Pliocene and preindustrial simulations (left plot) and the difference between the two (right plot). Note the separate scales on the X-axis. Changes in cloud cover at all heights are small, but they are consistent. Total cloud cover decreases throughout most of the troposphere and acts as a positive feedback to warming in the Pliocene simulation.